Role of Active Site Tyrosine Residues in Catalysis by Human Glutathione Reductase†

R. Luise Krauth-Siegel,*,‡ L. David Arscott,§ Annette Schönleben-Janas,‡ R. Heiner Schirmer,‡ and Charles H. Williams, Jr.§,⊥

Biochemie-Zentrum, Heidelberg University, 69120 Heidelberg, Germany, Department of Veterans Affairs Medical Center, Ann Arbor, Michigan 48105, and Department of Biological Chemistry, University of Michigan, Ann Arbor, Michigan 48109

Received March 19, 1998; Revised Manuscript Received July 6, 1998

ABSTRACT: Tyr114 and Tyr197 are highly conserved residues in the active site of human glutathione reductase, Tyr114 in the glutathione disulfide (GSSG) binding site and Tyr197 in the NADPH site. Mutation of either residue has profound effects on catalysis. Y197S and Y114L have 17% and 14% the activity of the wild-type enzyme, respectively. Mutation of Tyr197, in the NADPH site, leads to a decrease in K_m for GSSG, and mutation of Tyr114, in the GSSG site, leads to a decrease in K_m for NADPH. This behavior is predicted for enzymes operating by a ping-pong mechanism where both half-reactions partially limit turnover. Titration of the wild-type enzyme or Y114L with NADPH proceeds in two phases, E_{ox} to EH_2 and EH_2 to EH_2−NADPH. In contrast, Y197S reacts monophasically, showing that excess NADPH fails to enhance the absorbance of the thiolate−FAD charge-transfer complex, the predominant EH_2 form of glutathione reductase. The reductive half-reactions of the wild-type enzyme and of Y114L are similar; FAD reduction is fast (∼500 s^{-1} at 4 °C) and thiolate−FAD charge-transfer complex formation has a rate of 100 s^{-1}. In Y197S, these rates are only 78 and 5 s^{-1}, respectively. The oxidative half-reaction, the rate of reoxidation of EH_2 by GSSG, of the wild-type enzyme is approximately 4-fold faster than that of Y114L. These results are consistent with Tyr197 serving as a gate in the binding of NADPH, and they indicate that Tyr114 assists the acid catalyst His467′.

Glutathione reductase catalyzes the reduction of glutathione disulfide (GSSG)[1] at the expense of NADPH:

$$GSSG + NADPH + H^+ \rightleftharpoons 2GSH + NADP^+$$

By maintaining a high ratio of [GSH]/[GSSG], the enzyme enables several vital functions of the cell such as the detoxification of reactive oxygen species as well as protein and DNA biosynthesis (*1*).

Glutathione reductase is a member of the family of homodimeric FAD−disulfide oxidoreductases (*2*). The catalytic mechanism of the enzyme has been thoroughly investigated by spectroscopic, kinetic, and genetic approaches as well as by protein crystallography. The reducing equivalents are passed from NADPH to glutathione disulfide via the isoalloxazine ring of the prosthetic group FAD and the active site disulfide/dithiol couple. The catalytic cycle can be subdivided into two half-reactions. The first one represents the reduction of the enzyme by NADPH which results in the formation of EH_2, a stable equilibrium mixture of two-electron reduced species. The major species in EH_2, the thiolate−FAD charge-transfer complex, is characterized by oxidized FAD and an active site dithiol. The second half-reaction describes the reduction of GSSG by EH_2 and the concomitant regeneration of the oxidized enzyme E_{ox} with an active site disulfide (*2*−*5*).

Among the amino acid residues which are directly involved in catalysis, two tyrosines—Tyr114 in the GSSG binding site and Tyr197 in the NADPH binding site of GR—are highly conserved when glutathione reductases from different species are compared (Figure 1). The equivalent of Tyr114 is also found in the mechanistically related enzymes trypanothione reductase and thioredoxin reductase from higher organisms and in the bacterial mercuric ion reductase. In contrast, lipoamide dehydrogenase has a branched-chain amino acid residue. Tyr197 is found in all known glutathione reductases and in thioredoxin reductase from higher eukaryotes. In trypanothione reductases, Tyr or Phe occupies this position whereas in mercuric ion reductases and lipoamide dehydrogenases Tyr or a branched-chain residue is present (*2*).

† This research was supported by the Deutsche Forschungsgemeinschaft (Grants Kr 1242/1-3 and Schi 102/7-5) (R.L.K.-S., R.H.S.), by the Department of Veterans Affairs (C.H.W.), and by NIGMS Grant GM21444 (C.H.W.).

* To whom correspondence should be addressed at Biochemie-Zentrum Heidelberg, Ruprecht-Karls-Universität, Im Neuenheimer Feld 328, D-69120 Heidelberg, Germany. Phone 49-6221-54 41 74. Fax 49-6221-54 55 86.

‡ Heidelberg University.

§ Department of Veterans Affairs Medical Center.

⊥ University of Michigan.

[1] Abbreviations: DNPG, *S*-(2,4-dinitrophenyl)glutathione; E_{ox}, enzyme in the oxidized form; EH_2, enzyme in the two-electron reduced form; GR, human glutathione reductase (EC 1.6.4.2); GSSG, glutathione disulfide; GSH I, the moiety of GSSG which forms a mixed disulfide with GR; GSH II, the moiety which leaves the enzyme first during catalysis; GlyI and GlyII residues of the substrate GSSG; LipDH, lipoamide dehydrogenase (EC 1.8.1.4). Y114L, Y197S, and Y114L/Y197S designate the respective single or double mutations *and* also the mutant enzyme species. FAD in titration experiments represents enzyme-bound FAD or the enzyme subunit.

S0006-2960(98)00637-0 CCC: $15.00
Published on Web 09/12/1998

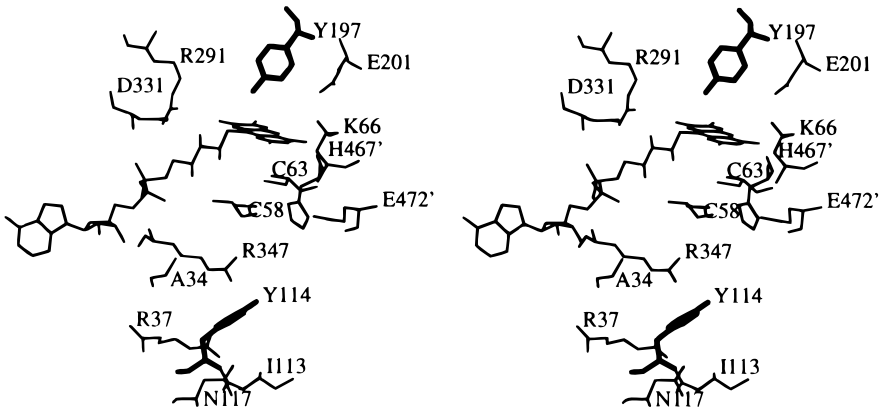

FIGURE 1: Stereoview of the active site of dimeric human glutathione reductase. The isoalloxazine ring of FAD forms the center of the active site and separates the binding sites for the two substrates (*5*). Cys58 and Cys63 represent the active site dithiol/disulfide. Glu472′ and His467′, the acid catalyst, are contributed by the other subunit. Tyr114 and Tyr197, which have been mutagenized to Leu and Ser, respectively, in the present work are depicted in bold lines. In the oxidized enzyme the side chain of Tyr197 points nearly perpendicularly onto the flavin. Binding of NADPH causes the side chain to turn around. In its new position the phenol ring is approximately parallel to the nicotinamide and flavin rings. Tyr114 points into the disulfide binding site and moves when GSSG binds to the enzyme (for details see Figure 2). The figure is based on the structural data of GR (*8*) deposited at the Protein Data Bank, Brookhaven (accession no. 3GRS). It has been kindly provided by Dr. Alfonso Martinez, Max-Planck-Institut für Medizinische Forschung, Heidelberg.

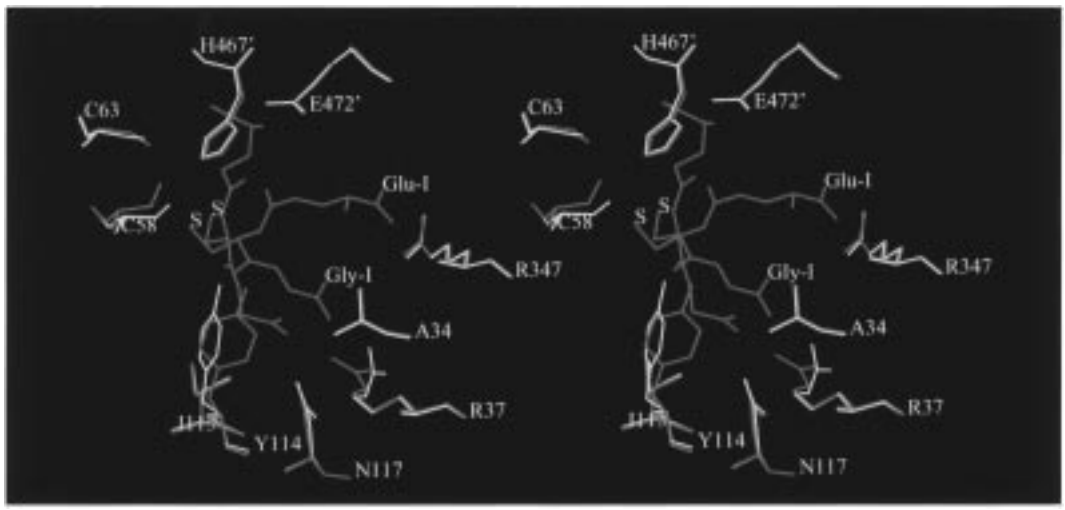

FIGURE 2: Superposition of the structures of EH_2 with the E−GSSG complex of human GR. The structure of the GR−NADH−inorganic phosphate complex (representing EH_2, yellow; PDB accession no. 1GRB) is superimposed with the structure of the GR−GSSG−$NADP^+$ complex (representing E−GSSG, blue; PDB accession no. 1GRA). Binding of GSSG (green) causes the side chain of Tyr114 to move by nearly 1 Å and to rotate around its $C_\beta - C_\gamma$ bond. In the enzyme−GSSG complex the oxygen of the OH group is 3.1 and 3.4 Å away from the peptide nitrogens of CysI and GlyII of GSSG, respectively. It points toward the disulfide with distances of 4.06 and 3.96 Å to the sulfurs of CysI and CysII of GSSG, respectively, and 2.8 Å from water 502. The figure was kindly provided by Dr. Alfonso Martinez (see legend of Figure 1).

Tyr114 and Tyr197 undergo pronounced movements when the respective substrate binds at the active site as shown by X-ray diffraction analysis of enzyme−substrate complexes (*5*−*8*). In the absence of GSSG, the side chain of Tyr114 points toward the position which in the GR−GSSG complex is occupied by the disulfide bridge of the substrate. Binding of GSSG causes the side chain to rotate and translate by nearly 1 Å from its original position (Figure 2). The hydroxyl group now points toward the sulfur atom of glutathione II and is in hydrogen-bonding distance to the main chain nitrogens of CysI and GlyII of GSSG (*6*).

In the unliganded enzyme, the side chain of Tyr197 points nearly perpendicularly onto the flavin ring. It has been suggested that this arrangement protects the enzyme from solvent access (*5*). Binding of NADPH causes Tyr197 to undergo a main chain motion and to rotate around its $C_\alpha - C_\beta$ bond, whereby the OH group moves by 6.4 Å (*6*). In the enzyme−NADPH complex, the flavin, the nicotinamide, and the Tyr197 rings are nearly parallel (*7*).

Here we report the kinetic, spectroscopic, and catalytic properties of human GR species in which Tyr114 or Tyr197 or both residues have been replaced by Leu and Ser, respectively. The data presented show that these aromatic residues at the substrate binding sites of the enzyme play a crucial role for the catalytic efficiency and specificity of GR.

MATERIALS AND METHODS

Materials. For expression of recombinant wild-type and mutant hGR species, *Escherichia coli* SG5 cells were used which have a chromosomal deletion of the *gor* gene coding for glutathione reductase (*9*). The vector containing hGR cDNA adapted for overexpression in *E. coli* SG5 cells is pUB302-2 (*10*). The mutagenic oligonucleotides were prepared on an ABI DNA synthesizer: 5′ GAGATTGT-

TCTGCAGGATGGCATTC 3′ (Y114L) and 5′ CATCTCCACAGCAATCGATCCTGCACCAACAAT 3′ (Y197S). For identification of the expected cDNA mutants an extra *Pst*I site (Y114L) and an extra *Cla*I site (Y197S) were generated in the oligonucleotides. The *Cla*I site was found to be ineffective, probably due to methylation of adenine at N^6 in the sequence GATC.

A sample of *S*-(2,4-dinitrophenyl)glutathione was kindly provided by Drs. Theo Akerboom and Helmut Sies, Düsseldorf. Thio-$NADP^+$ was purchased from Sigma. All other reagents (from Boehringer, Serva, Sigma, Biomol) were of the highest available purity.

Construction of the Mutants. The two single tyrosine mutants were obtained by site-directed mutagenesis using wild-type hGR cDNA as a template. The hGR-encoding *Eco*RI/*Hin*dIII fragment (noncoding strand) of the expression plasmid pUB302-2 was subjected to mutagenesis according to the method of Kunkel (*11*) using the Bio-Rad kit. Putative mutants were screened by restriction site analysis. The mutation was confirmed by dideoxy sequencing (*12*) of the entire coding region.

The Y114L/Y197S double mutant was constructed by digestion of the plasmids carrying Y114L and Y197S with *Xma*III, which results in two fragments in each case. The small fragment represents part of the 5′ end of the gene including the region coding for Y114, whereas the large fragment consists of the 3′ fragment of the gene with the Y197 containing sequence and the vector. The small fragment containing the Y114L coding region and the large vector fragment containing the Y197S coding region were isolated. Ligation of the two fragments resulted in the Y114L/Y197S double mutant. The mutations were confirmed by DNA sequencing.

Protein Determination. In crude fractions, an absorption of 1 at 280 nm was assumed to correspond to a protein concentration of 1 mg/mL. In solutions of purified GR, the protein concentration was determined by means of the flavin absorption using an absorption coefficient at λ_{max} of 11.3 mM^{-1} cm^{-1} for E_{ox}.

Measurement of Kinetic Parameters. Specific activities of wild-type and mutant glutathione reductases were measured under substrate saturating conditions in 47 mM potassium phosphate, 200 mM KCl, and 1 mM EDTA, pH 6.9 at 25 °C (GR assay buffer) (*13*−*14*). The specific activity of human GR tends to increase by up to 50% when the protein is stored over months at 4 °C in the presence of low molecular weight thiols. All enzyme used in the present studies was fully active.

The oxidase activity of GR is defined as the rate of NADPH oxidation in the absence of GSSG under aerobic conditions. Transhydrogenase activity was measured with thio-$NADP^+$ as an electron acceptor at 30 °C (*15*). The assay mixture contained 100 μM NADPH and 100 μM thio-$NADP^+$ in 100 mM potassium phosphate, pH 7.6. The absorption increase due to thio-NADPH formation was followed at 395 nm ($\epsilon = 11.3$ mM^{-1} cm^{-1}).

Inhibition of the Mutant hGR Species by S-(2,4-Dinitrophenyl)glutathione (DNPG). A 10 mM stock solution of DNPG was prepared in GR assay buffer. Inhibition of wild-type and mutant GR species was followed at constant concentrations of 100 μM NADPH and 50 μM GSSG, varying the concentration of DNPG.

Purification and Crystallization of the Recombinant Mutant GR Species. Wild-type and mutant human GR species were produced in *E. coli* SG5 cells and purified by affinity chromatography on 2′,5′-ADP−Sepharose as described (*10*). Y114L and Y197S GR were crystallized by vapor diffusion. Using the hanging drop procedure, microcrystals ($50 \times 50 \times 50$ μm^3) were grown from a 5 mg/mL protein solution in GR assay buffer containing 0.4 M ammonium sulfate within a few days. The ammonium sulfate concentration in the reservoir varied between 0.6 and 1 M.

Spectroscopy. Fluorescence emission spectra of wild-type, Y114L, and Y197S human GR were recorded in GR assay buffer without EDTA; the excitation wavelength was 450 nm. Absorption spectra were recorded on a Hitachi 150-20 spectrophotometer or a Milton Roy Spectronic 3000 diode array spectrophotometer.

Rapid Reaction Kinetics. The rapid kinetics were followed at 4 °C in an anaerobic stopped-flow spectrophotometer designed by L. D. Arscott and D. P. Ballou, University of Michigan, as described by Rietveld et al. (*16*).

Redox Potentials. The redox potentials of wild-type and mutant GR species were determined by equilibrating the enzyme with NAD^+/NADH (*17*). E_{ox} in GR assay buffer of pH 6.9 was titrated at 25 °C with NADH in the presence of a 100-fold molar excess of NAD^+ over enzyme subunit. The concentration of free NADH was calculated from the change in absorption at 358 nm using an ϵ of 4400 M^{-1} cm^{-1}. At this wavelength E_{ox} and EH_2 are isosbestic. Formation of EH_2 was followed at 540 nm, the extinction coefficients being 2450, 2400, and 2660 M^{-1} cm^{-1} for Y197S, Y114L, and the wild-type enzyme, respectively. E_m for the NAD^+/NADH couple under the conditions used is −312 mV (*18*). The following equations were applied:

$$K_{eq} = \frac{[EH_2][NAD]}{[E_{ox}][NADH]}$$

$$[E_{ox}] = [E_{total}] - [EH_2]$$

$$[NAD_{formed}] = [EH_2]$$

$$[NAD] = [NAD_{initial}] + [NAD_{formed}]$$

RESULTS

Enzymatic Activities of Y197S, Y114L, Y114L/Y197S, and Wild-Type Human GR. Replacement of Tyr197—which is located in the NADPH binding site of GR (Figure 1)—by a Ser residue does not influence the K_m value for NADPH but significantly lowers the K_m value for GSSG (Table 1). This observation provides valuable insight into the kinetic mechanism of the mutant protein. As outlined by Matthews (*19*), a mutation which alters the ratios of the catalytic velocities of the individual half-reactions of an enzyme with a ping-pong mechanism can be expected to decrease the K_m value for the substrate in the half-reaction that becomes less rate limiting as a result of the altered catalytic activity of the mutant enzyme. The rapid reaction kinetics of the reductive half-reaction of Y197S (see below) are in agreement with these theoretical considerations.

In contrast to the physiologic disulfide reductase activity—which is only 14% that of wild-type GR—the transhydro-

Table 1: Kinetic Parameters of Wild-Type and Mutant Human GR Species[a]

parameter	wild type	Y114L	Y197S	Y114L/ Y197S
K_m values (μM)				
NADPH	7 ± 1	2 ± 0.3	7 ± 1	2 ± 0.2
GSSG	65 ± 5	300 ± 10	17 ± 3	200 ± 10
specific activities [unit(s)/mg]				
GSSG reductase	200 ± 20	30 ± 5	27 ± 3[b]	9 ± 1
oxidase	≤ 0.01	0.005	0.019	0.024
transhydrogenase[c]	0.15	0.04	1.5	1.4
activity ratios				
GSSG reductase/oxidase	>20000	6000	1400	370
GSSG reductase/ transhydrogenase	1300	750	18	6.4
inhibition by DNPG[d]				
IC_{50} values	30	40	≥ 500	≥ 500

[a] GSSG reductase and the oxidase activity were measured in GR assay buffer, pH 6.9 at 25 °C. The apparent K_m values for GSSG were determined in the presence of 100 μM NADPH and those for NADPH in the presence of 1 mM GSSG. [b] Because of the pronounced substrate inhibition of the Y197S mutant, the specific activity at 200 μM GSSG is given. [c] The transhydrogenase activity was measured at fixed concentrations of 100 μM NADPH and thio-$NADP^+$ in 100 mM potassium phosphate, pH 7.6 at 30 °C. Since the transhydrogenase activity of yeast GR is known to be sensitive to substrate inhibition and to the ionic composition of the assay medium (*15*), the values should be used only for the direct comparison of the four human GR species under these fixed assay conditions. [d] Inhibition by DNPG is given at constant concentrations of 100 μM NADPH and 50−60 μM GSSG.

genase and oxidase activities are increased in the Y197S mutant. The resulting lower ratios of reductase to transhydrogenase and oxidase activities, respectively, indicate that Tyr197 plays a role in the catalytic specificity of GR. During catalysis, Tyr197 undergoes a substantial conformational change. In the absence of the nicotinamide cofactor, the side chain of Tyr197 points perpendicularly onto the flavin ring, covering it as a protective lid. Binding of NADPH causes the side chain to move away to open the pocket for the incoming nicotinamide (*6*). In Y197S the small hydrophilic side chain at this position gives rise to a more open binding site which may allow for easier access of molecular oxygen or thio-$NADP^+$ to the flavin; this would lead to a decreased substrate specificity of the mutant protein.

Substitution of Tyr114 in the GSSG binding site of GR by a leucine residue reduces the physiological GSSG reductase activity to 17% that of wild-type GR, approximately to the same extent as the Y197S mutant. The Tyr114 mutation leads to a similar phenomenon, that is, a decrease of the K_m for NADPH (Table 1). Indeed, this mutation of a residue at the disulfide substrate binding site is expected to decrease the K_m value for the substrate in the first half-reaction provided this reaction becomes less rate limiting in the mutant enzyme (see below) (*19*). Replacement of both tyrosine residues in the Y114L/Y197S mutant causes a further decrease of the specific activity to only 5% when compared to wild-type GR.

DNPG Inhibits Y114L and Wild-Type GR but Not Y197S and Y114L/Y197S. DNPG—a conjugate which is formed in the reaction of 1-chloro-2,4-dinitrobenzene with glutathione—is an inhibitor of human GR *in vitro* and *in vivo*. As shown by X-ray crystallography, the major binding site of DNPG overlaps with the binding site of the substrate GSSG, whereby binding of the inhibitor causes a movement of the side chain of Tyr114 (*20*). Since DNPG has an additional binding site in a cavity at the 2-fold axis of the homodimeric protein, the inhibition pattern is not interpretable by classical mechanisms. In the presence of saturating concentrations of NADPH and a GSSG concentration that corresponds approximately to the wild-type GR K_m value of the disulfide substrate, DNPG inhibits GR with an IC_{50} value of 30 μM. Mutation of Tyr114 into a leucine gives an enzyme having the same inhibition pattern as is observed in the wild-type enzyme with an IC_{50} value of 40 μM. In contrast, Y197S and Y114S/Y197L are much less inhibited by DNPG, the IC_{50} values being higher than 500 μM. Besides the impaired interaction of Y197S with this effective inhibitor of wild-type GR, the mutant shows a pronounced inhibition by its substrate GSSG. X-ray diffraction analysis of Y197S will reveal whether structural alteration at the GSSG binding site contributes to these effects. Crystals of $50 \times 50 \times 100$ μm^3 have already been grown.

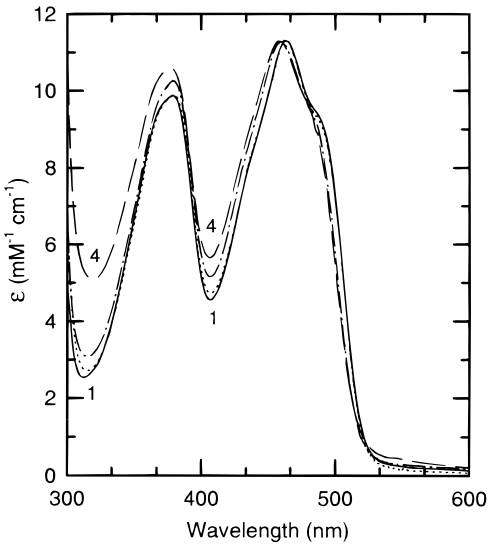

FIGURE 3: Visible absorption spectra of wild-type GR, Y114L, Y197S, and Y114L/Y197S. The spectra were recorded in GR assay buffer, pH 6.9 at 25 °C, under anaerobic conditions. The λ_{max} values are blue shifted by 2 nm when compared to spectra under aerobic conditions (Table 2). The spectra are as follows: 1, wild-type GR; 2, Y114L; 3, Y197S; 4, Y114L/Y197S.

Spectral Characteristics of the Oxidized and Two-Electron Reduced Enzyme Species. The visible absorption spectra of wild-type and mutant GR species are shown in Figure 3. Y114L has a spectrum which is nearly indistinguishable from that of the wild-type enzyme. The tyrosine residue in the GSSG binding site does not directly interact with the flavin (Figures 1 and 2). In contrast, substitution of Y197 by a Ser residue causes a 5 nm blue shift and a flattening of the shoulder of the visible absorption maximum, in agreement with the more hydrophilic environment of the flavin in the mutant protein (Table 2).

Anaerobic titration of Y114L, Y197S, and wild-type GR by up to 1 equiv of NADPH resulted in the formation of EH_2, the mixture of two-electron reduced enzyme forms (Table 3). The thiolate−FAD charge-transfer complex, the predominant species at the EH_2 reduction level of GR in static titrations, is characterized by a broad absorption band around 540 nm due to the charge-transfer interaction between Cys63 and the flavin (Table 2) (*21*). The spectra generated

Table 2: Spectral Characteristics of Oxidized and Two-Electron Reduced Human GR Species[a]

	wild type	Y114L	Y197S
E_{ox}, λ_{max} visible (nm)	463	463	458[b]
ϵ_{540nm} (M^{-1} cm^{-1})			
thiolate−FAD charge-transfer complex	2500	2200	3200
thiolate−FAD charge-transfer complex (with NADPH bound)	4300	4000	3500
$\lambda_{max,}$ fluorescence emission (nm)	520	520	520
quantum yield, relative to free FAD (%)	<2	<2	20

[a] Wild-type and mutant GR species were titrated anaerobically with NADPH in GR assay buffer, pH 6.9 at 25 °C. The extinction coefficients for EH_2 and EH_2−NADPH at 540 nm represent the spectral data at 1 equiv and excess NADPH, respectively. The fluorescence emission spectra were recorded in GR assay buffer, pH 6.9, without EDTA. [b] Y114L/Y197S has the same visible λ_{max} as Y197S.

Table 3: Spectrally Distinguishable Two-Electron Reduced Species of GR Listed in Order of Appearance in the Reaction Mechanism (*19*)

charge-transfer complexes	characteristic wavelength (nm)	ref
NADPH−FAD	570	*16*
$FADH^-$−$NADP^+$	670	*16*
thiolate−FAD	540	*21*
thiolate−FAD (with $NADP^+$ bound)	600	*22*
thiolate−FAD (with NADPH bound)	540	*22*

during this phase of the titration are isosbestic at 510, 430, 400, and 360 nm. In wild-type GR and in Y114L, more than 1 equiv of NADPH causes a continuous decrease of the flavin absorption at 460 nm and an increase at 350 nm. The absorption at 540 nm increases also due to enhancement of the thiolate−FAD charge-transfer complex by NADPH (Tables 2 and 3). In this phase the isosbestic wavelengths are 500 and 380 nm, clearly distinct from those observed in the first phase. Thus, reduction of E_{ox} to EH_2 is spectrally distinct from complex formation, EH_2 to EH_2−NADPH.

The thiolate−FAD charge-transfer complex of Y197S is enhanced only slightly in the presence of excess NADPH (Table 2). No clear isosbestics are observed in the titration beyond 1 equiv of NADPH per FAD. This indicates that in the absence of the tyrosine the thiolate−FAD charge-transfer complex does not interact with the nicotinamide ring of NADPH. In the crystal structure of the EH_2−NADPH complex of wild-type GR, the side chain of Y197 is nearly parallel to the flavin and nicotinamide ring systems (*6*). It covers the back (*re*) side of the nicotinamide and thus may hold the nicotinamide in position for specific interaction with the flavin.

Fluorescence Behavior of Wild-Type and Mutant GR Species. Excitation of the flavin in wild-type human GR at 450 nm results in a very low emission at 520 nm (Table 2). The extensive quenching has been attributed to a dynamic mechanism with enhanced flexibility of the flavin (*23*).

The fluorescence emission spectrum of Y114L is essentially the same as that of wild-type GR with a typical shoulder around 545 nm. In contrast, Y197S lacks the shoulder, and it exhibits a much higher quantum yield, namely, about 20% of that observed for free FAD. A role of Tyr197 in quenching the flavin fluorescence in GR agrees well with the properties of a mutant of *E. coli* lipoamide dehydrogenase. In wild-type LipDH, which has a much higher flavin fluorescence than GR (*23*), Ile184 occupies the position equivalent to Tyr197 in GR. Replacement of the aliphatic residue by a Tyr resulted in a protein species with spectral properties closely resembling those of GR; the FAD fluorescence, for instance, was nearly completely quenched (*24*). In agreement with these data, replacement of Tyr177 by Phe, Ser, or Gly in *E. coli* GR causes a strong increase in flavin fluorescence (*25*).

Table 4: Rate Constants of the Reductive and Oxidative Half-Reactions

	obsd wavelength (nm)	reductive		oxidative		
		k_{1app} (s^{-1})	k_{2app} (s^{-1})	k_{3app} (s^{-1})	k_{4app} (s^{-1})	phases[a]
wild type	463	>500	100	45		3
	540			51		2
Y114L	463	>500	100	78	11	4
	540			12	14	3
Y197S	463	78	5	60	3	2
	540		5	ND[b]	ND[b]	ND[b]

[a] Minimal number of exponential equations fitting the observed kinetic traces. [b] Not determined due to insufficient thiolate−FAD charge transfer to measure.

Redox Potentials of Y114L, Y197S, and Wild-Type Human GR. The redox potentials of the E_{ox}/EH_2 couple of wild-type and mutant GR were determined by equilibration with NAD/NADH. The nonphysiologic substrate NADH was chosen as a reductant since EH_2 forms a stable complex with NADPH, which would interfere with the measurement of EH_2 at 540 nm (*2*). The redox potentials obtained at pH 6.9 and 25 °C (−229 ± 4 mV for wild-type GR; −228 ± 4 mV for Y114L, and −224 ± 2 mV for Y197S, respectively) were found to be the same within standard deviations, which indicates that the active site tyrosines do not influence the redox states of the enzyme.

The Reductive Half-Reaction. The reactions of NADPH with wild-type GR, Y114L, and Y197S were characterized (Table 4). This half-reaction is essentially the same for wild-type GR and Y114L and gives a kinetic trace which can be fitted to the sum of three exponential equations. The first step, NADPH binding to oxidized enzyme to form the NADPH−FAD charge-transfer complex, is observed as a small but immediate decrease at 463 nm and an increase at 570 nm (Table 3). Formation of the complex is virtually complete within the dead time of the instrument (3 ms) and thus is not measured directly. The first exponential phase, observed as an additional decrease at 463 nm and an increase at 670 nm, can be ascribed to electron transfer within the NADPH−FAD charge-transfer complex to form the $FADH^-$−$NADP^+$ charge-transfer complex (Table 3). The rates measured at these two wavelengths appear to be linearly dependent on the concentration of NADPH for at least 4 equiv of NADPH per FAD. A plot of these rates (data not shown) as a function of the NADPH concentration yields a slope corresponding to a second-order rate constant of 4.7×10^6 M^{-1} s^{-1} and 5.8×10^6 M^{-1} s^{-1} for wild-type GR and Y114L, respectively, well within the accepted range for enzymatic second-order rate constants that are not diffusion controlled. The line intercepts the rate axis at 170 s^{-1}, and it is suggested that this rate represents a reverse reaction, perhaps the dissociation of NADPH from the enzyme (*26*, *27*). At 10 equiv of NADPH, the rate of the first phase falls

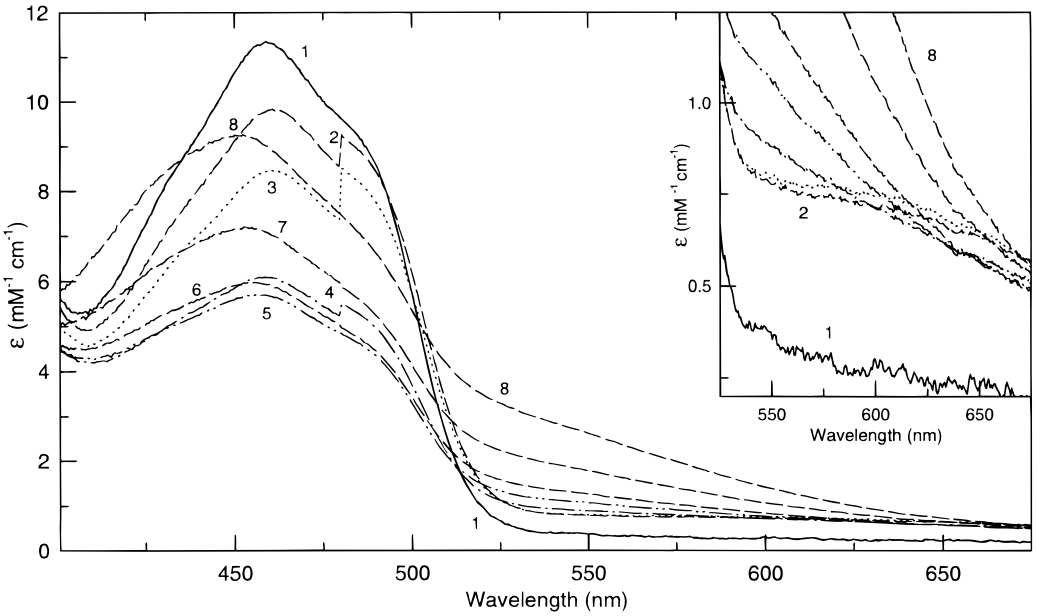

FIGURE 4: Spectra collected during reduction of Y197S by NADPH. Enzyme was mixed (16.5 μM final concentration) in the rapid reaction spectrophotometer with 1 equiv of NADPH in an equal volume of GR assay buffer, pH 6.9 at 4 °C. Times for each spectrum are as follows: 1, oxidized; 2, 8 ms; 3, 13 ms; 4, 35 ms; 5, 63 ms; 6, 90.5 ms; 7, 170 ms; 8, 496 ms. Spectra were recorded from the diode array detector following the 2.5 ms dead time beginning at ca. 480 nm and scanning to higher wavelengths ending at ca. 479 nm 5.5 ms later, which results in the discontinuity in the 8, 13, and 35 ms spectra. Inset: The data at longer wavelengths have been expanded to show a small amount of the remaining NADPH−FAD charge-transfer complex and the $FADH^-$−$NADP^+$ charge-transfer complex (spectra 2 and 3).

significantly below the line for both wild-type GR and Y114L, thus making interpretation of the first exponential phase more complex. This behavior has not been observed with GR from any other organism (*16*, *28*). Thus, lacking sufficient pre-steady-state rate data and species characteristics (e.g., extinction coefficients) which could aid in modeling this reductive half-reaction, we have chosen to represent this first phase as being faster than 500 s^{-1} (Table 4). The second phase is independent of the NADPH concentration, occurs at a rate of approximately 100 s^{-1} (k_2), and represents reduced flavin reoxidation concurrent with disulfide reduction to the thiolate−FAD charge-transfer complex (Table 3). The third and final exponential phase proceeds with rates between 0.5 and 6 s^{-1} (not shown in Table 4) and cannot be ascribed to any specific species except perhaps a final equilibrium readjustment between the binding of excess NADPH and the product, $NADP^+$, to EH_2.

In contrast, the rate of FAD reduction of Y197S was found to be slow by comparison with the rate for wild-type GR and Y114L. There were only two phases; the first had a maximal rate (at saturating NADPH concentrations) of 78 s^{-1} with a $K_{d(app)}$ of 6.7 μM which was attributed to the binding of NADPH to the enzyme (*26*). The subsequent conversion to the thiolate−FAD charge-transfer complex was also slow (5 s^{-1}) and NADPH independent. Spectra collected during the reduction showed that very small amounts of the NADPH−FAD charge-transfer complex observed at 570 nm and the $FADH^-$−$NADP^+$ charge-transfer complex followed at 670 nm were maximal between 8 and 13 ms while flavin reduction continued up to 60 ms (Figure 4 and Table 3). Given the close interaction between Tyr197, the nicotinamide ring, and the flavin in wild-type GR, it is of significance that the oxidation of the flavin to give the thiolate−FAD charge-transfer complex (a first-order reaction) was also markedly slowed by the Y197S mutation to a rate of 5 s^{-1}. During the flavin reoxidation the wavelength maximum shifted from 460 to 450 nm (Figure 4) as has been observed in *E. coli* glutathione reductase (*16*).

The Oxidative Half-Reaction. Two-electron reduced enzyme species were obtained by reduction of Y114L with sodium borohydride. However, the EH_2 forms of Y114L were not stable over hours. Therefore, the oxidative half-reaction was studied as part of a single turnover. Preliminary experiments had shown that the rates of the oxidative half-reaction measured rapidly with borohydride reduced Y114L or in turnover are very nearly the same.

The enzymes (wild-type GR, Y114L or Y197S) in one syringe were mixed with a solution containing 1 equiv of NADPH and varying concentrations of GSSG. Thus, the reductive half-reaction was observed prior to reoxidation of the enzyme by GSSG (Table 4). Because 1 equiv of $NADP^+$ is present during reoxidation, a small amount is bound to the enzyme. To the extent that the binding constant for $NADP^+$ to EH_2 varies among wild-type enzyme and Y114L, the rates of reoxidation will be less than perfectly comparable. Figure 5 shows spectra collected during the course of a single turnover for the wild-type enzyme. Spectrum 3 at 13 ms indicates the highest transient yield of the NADPH−FAD charge-transfer complex and the $FADH^-$−$NADP^+$ charge-transfer complex (Table 3). Spectrum 4 at 27 ms gives the highest level of thiolate−FAD charge-transfer complex (inset, 540 nm); its further formation is obscured by reoxidation at a rate of 20 s^{-1} at 1 equiv of GSSG. Spectrum 5 at 89 ms represents approximately 50% reoxidation of the thiolate−FAD charge-transfer complex, and spectrum 6, at 300 ms, shows the final equilibrium mixture which approaches the spectrum of the oxidized enzyme. The maximal rate of the reoxidation of EH_2 in wild-type GR by GSSG is 45−51 s^{-1} (Table 4). The $K_{d(app)}$ of the EH_2−GSSG complex is 21−30 μM.

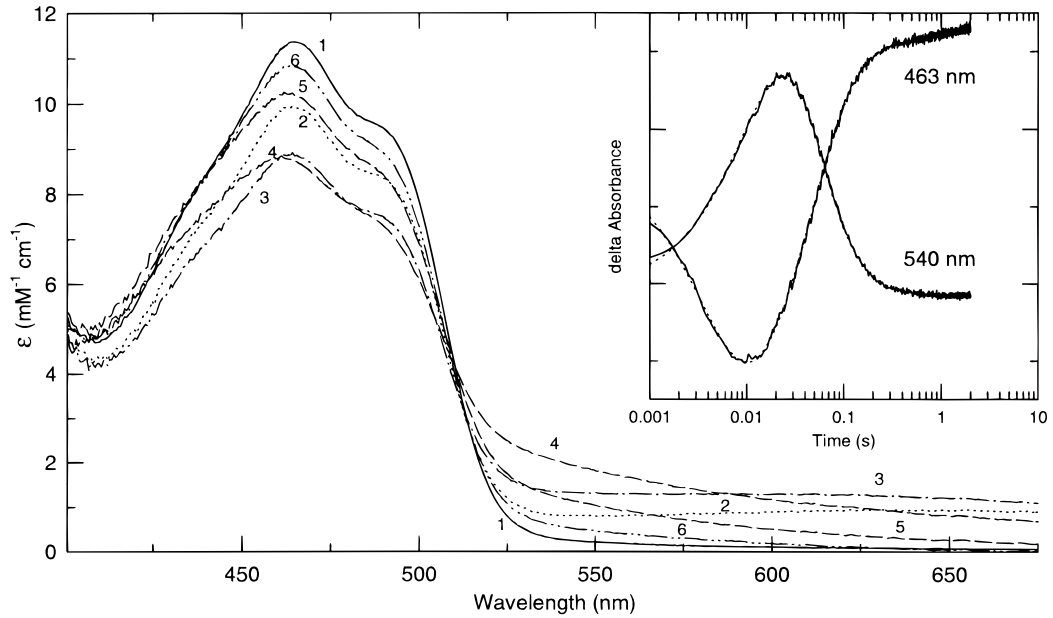

FIGURE 5: Spectral changes of wild-type GR during a single turnover. Enzyme (17.4 μM after mixing) was mixed in the rapid reaction spectrophotometer with 1 equiv of NADPH per FAD + 1 equiv of GSSG in an equal volume of GR assay buffer, pH 6.9 at 4 °C. Times for each spectrum are as follows: 1, oxidized; 2, 8 ms; 3, 13 ms; 4, 29 ms; 5, 89 ms; 6, 300 ms. Inset: The time course of the reaction at the indicated wavelengths is shown for the first 2 s of the reaction. The fitted curves, the sum of three exponentials for A_{463nm} and two exponentials for A_{540nm}, are shown as dots. Full-scale absorbance is 0.05 for both A_{463nm} and A_{540nm}.

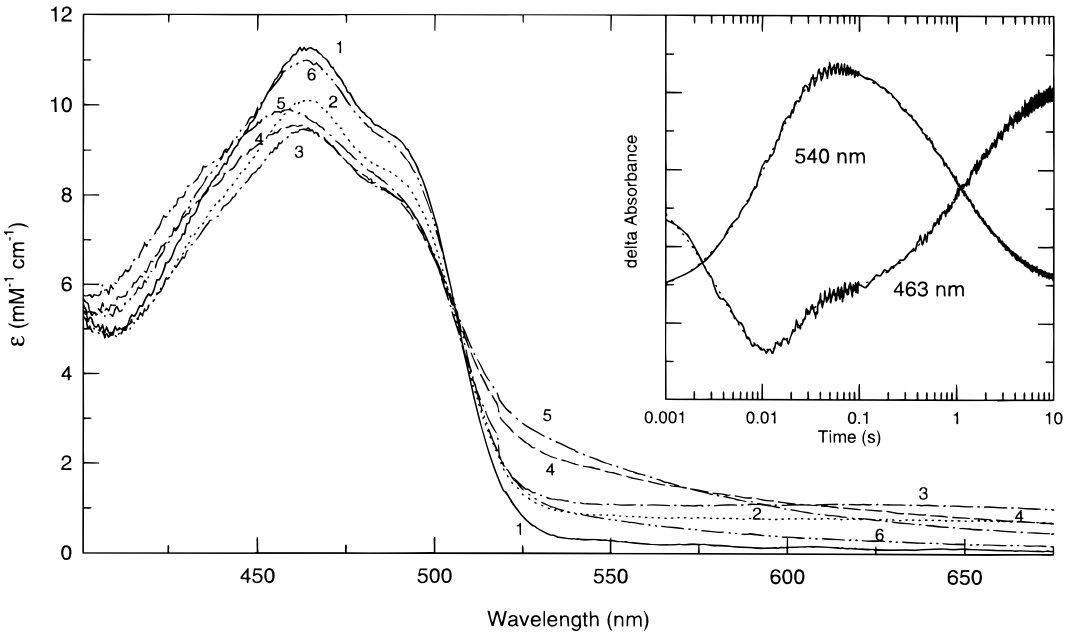

FIGURE 6: Spectral changes of Y114L during a single turnover. Enzyme was mixed (19.5 μM final concentration) in the rapid reaction spectrophotometer with 1 equiv of NADPH per FAD + 1 equiv of GSSG in an equal volume of GR assay buffer, pH 6.9 at 4 °C. Times for each spectrum are as follows: 1, oxidized; 2, 8 ms; 3, 13 ms; 4, 29 ms; 5, 89 ms; 6, 27.4 s. Inset: The time course of the reaction at the indicated wavelengths is shown for the first 10 s of the reaction. The fitted curves, the sum of four exponentials for A_{463nm} and three exponentials for A_{540nm}, are shown as dots. Full-scale absorbance is 0.05 for both A_{463nm} and A_{540nm}.

The rate of reoxidation of Y197S would presumably be the same as the rate for the wild-type enzyme (45−51 s^{-1}) since this mutation should not influence the oxidative half-reaction. However, the rate of reoxidation in this turnover experiment is limited by the rate of reduction which is impaired in this mutant. Therefore, the two observed rates of 60 and 3 s^{-1} are limited by the preceding steps in the reductive half-reaction of 78 and 5 s^{-1} (Table 4).

The reoxidaton of Y114L by GSSG is slower than that of the wild-type enzyme. Spectra collected during the course of a single turnover for Y114L are shown in Figure 6, and the single wavelength kinetics are given in the inset. The notable difference between Y114L and wild-type GR is most conspicuous at 1, 2, and 3 equiv of GSSG per FAD where the reaction of Y114L, followed at 463 and 540 nm, shows an additional phase (cf. the insets of Figures 5 and 6). It is suggested that this phase is associated with the formation of a mixed disulfide intermediate, which is expected to accumulate when the GSSG concentrations are low. The observed rate at 463 nm, k_3, decreases slightly as the [GSSG]

increases, the average rate being $78 \pm 9\ s^{-1}$. Formation and decay of the mixed disulfide have been studied extensively in GR from yeast (*29*). As a result of this additional phase, reoxidation of the enzyme is limited by k_3 in wild-type GR and by k_4 in Y114L (Table 4). Aside from this detail, the patterns of single turnover with Y114L and wild-type GR are remarkably similar except that the rate of reoxidation is slower for the mutant enzyme (Table 4).

DISCUSSION

The isoalloxazine ring of the prosthetic group FAD separates the binding sites for the two substrates in GR and in related pyridine nucleotide−disulfide oxidoreductases. NADPH binds on the *re* side and GSSG on the *si* side. A highly conserved tyrosine residue is part of each binding site, Tyr197 and Tyr114, respectively, in the human enzyme (Figures 1 and 2). The small but significant movement of Tyr114 upon binding of GSSG and the large conformational change of Tyr197 upon binding of NADPH have been noted in crystallographic studies for some time (*5*, *30*, *31*). Tyr197 moves aside to allow the nicotinamide ring to assume its position parallel to the isoalloxazine ring; the phenol ring adopts a position parallel to the nicotinamide. An extensive π overlap is then possible among the three stacked rings. Glutathione reductase from yeast or *E. coli* at the EH_2 level binds NADPH strongly. The bound NADPH enhances the absorbance of the thiolate−FAD charge-transfer interaction (*21*, *22*). The data in Table 2 show that this is also true for the human enzyme. Alteration of Tyr197 markedly diminishes the absorption increase. In the absence of the phenol ring, the π overlap between the nicotinamide and isoalloxazine rings must be less efficient. These results indicate that Tyr197 not only protects the flavin from solvent access in the oxidized enzyme—as indicated by the crystal structure of the protein—but also plays a role in stabilizing the EH_2−NADPH complex. This confirms the suggestion that Tyr197 acts as a "spring" (*7*).

Relative to wild-type GR, the flavin absorption of Y197S in the E_{ox} form is blue shifted, the characteristic shoulder is less pronounced, and the mutant shows a strong increase in FAD fluorescence (Figure 3, Table 2). While in wild-type human GR the flavin fluorescence is almost completely quenched, Y197S shows an emission yield of 20% when compared to free FAD. Analogous observations have been reported for *E. coli* GR in which Tyr177 (corresponding to Y197 in the human enzyme) was replaced by a Phe, Ser, or Gly residue (*25*). All three mutant *E. coli* proteins had about 40% of the fluorescence intensity of free FAD. In a complementary experiment Ile184 in *E. coli* lipoamide dehydrogenase was substituted by a Tyr. The alteration caused a dramatic drop of the flavin fluorescence which was then comparable to that of wild-type GR (*24*). These results support the concept that quenching of the flavin fluorescence which is often observed in flavoproteins is mainly due to the correct juxtaposition of the flavin to aromatic amino acid residues.

The role of Tyr114 as GSSG binds is subtle. Glutathione reductase from virtually all species, trypanothione reductase, thioredoxin reductase from higher eukaryotes, and mercuric ion reductase all catalyze the dehydrogenation of NADPH and all have a tyrosine at the position equivalent to position 114 in human glutathione reductase. In contrast, lipoamide dehydrogenase, another member of the pyridine nucleotide−disulfide oxidoreductase family of flavoenzymes, catalyzes the reduction of NAD^+ in its physiological role and has an isoleucine residue at the corresponding position (*2*). Almost nothing is known concerning the intrinsic factors that influence the direction of catalysis. The removal of NADH by the electron transport chain is an extrinsic factor in lipoamide dehydrogenase catalysis (*32*), but it is reasonable to suppose that the enzyme structures influence the microscopic equilibria that determine the net flux of reducing equivalents favoring NADPH oxidation or NAD^+ reduction, respectively.

The movement of Tyr114 upon GSSG binding occurs in such a way that the phenolate oxygen can make hydrogen bonds to the main chain nitrogens of CysI and GlyII of GSSG (Figure 2). Hydrogen bonding to both amides would be favorable if the phenol were deprotonated. Bound water 502 is 2.8 Å from the phenolate oxygen. It is tempting to speculate that the phenolate could promote the protonation of GS^- II by the acid catalyst, His467′. It has been proposed that this protonation disfavors the reversibility of the mixed disulfide formation between the interchange thiol Cys58 and GSH I, yielding glutathione II as a free thiolate (*33*). Thus, the protonation of GS^- II, effected by His 467′ and promoted by Tyr114, would be a major factor in keeping catalysis moving toward GSH formation. It may be helpful to contrast this process in glutathione reductase, where the histidine and tyrosine residues are thought to act together as an acid catalyst, with catalysis by lipoamide dehydrogenase, where the histidine residue alone acts as a base catalyst. In glutathione reductase, GSSG reacts with EH_2 (histidine residue probably protonated), whereas in lipoamide dehydrogenase, dihydrolipoamide binds to E_{ox} (histidine residue unprotonated). Moreover, the product of the glutathione reductase reaction is two molecules of a monothiol, while in lipoamide dehydrogenase, the substrate is one molecule of a dithiol.

An alternate mechanism for rate enhancement has been considered, namely, polarization of the disulfide bond of GSSG or of the mixed disulfide by the phenolate oxygen (*35*, *36*). The phenolate is not positioned well with respect to the disulfide of GSSG, and the phenolate is at the wrong end of the mixed disulfide bond for such catalysis. Substitution of Y99 in *E. coli* GR (the equivalent of Y114 in the human enzyme) by a phenylalanine residue results in a mutant protein with catalytic properties very similar to those of the wild-type bacterial enzyme (*34*). This means either that a trapped H_2O molecule in the mutant can adopt the function of the phenolic OH group or that residue 99 may promote the dissociation of glutathione II by another mechanism. Regardless of the mechanism, the dissociation of GSH must require active participation of the enzyme considering the intracellular ratio of GSH to GSSG of approximately 100 (*1*). In this context it is of interest that also in glutathione *S*-transferases an essential tyrosine interacts with GSH (*37*, *38*).

Steady-State Kinetics. Y197S and Y114L have significantly lower specific activities than the wild-type enzyme (Table 1). In contrast, the very low oxidase and transhydrogenase activities of human GR are either not decreased or slightly increased in the mutant proteins. *E. coli* GR

species in which Y177 (Y197 of human GR) was replaced by a Phe, Ser, or Gly residue also showed a faster oxidation of the reduced enzyme species (*25*). These observations indicate that the tyrosine residues in the substrate binding sites play a role in the catalytic specificity of GR.

Each of the two Tyr mutations causes a lowering of the K_m value for the substrate in the opposite substrate binding site (Table 1). In an enzyme that follows a kinetic ping-pong mechanism, the K_m values are a function of the rate constants for both half-reactions. As shown by Matthews (*19*) a mutation which alters the ratios of the catalytic velocities of the individual half-reactions is expected to cause a decrease of the K_m value for the substrate in the half-reaction that becomes less rate limiting as a result of the altered catalytic activity of the mutant enzyme. For the comparison between wild-type GR (K_m for NADPH = 7.0 μM) and Y114L (K_m for NADPH = 2.0 μM), the prediction that the oxidative half-reaction is slower in the mutant was borne out by rapid reaction kinetics where the decrease in rate was 3.5-fold (see Table 4). Also with the Y197S mutant (exhibiting a lower K_m value for GSSG), a lowered rate constant for the reductive half-reaction as predicted according to ref *19* was confirmed experimentally. Similar observations have been made in *E. coli* GR. Replacement of His439′ (His467′ in human GR) by a Gln in the GSSG binding site causes a sharp drop of the K_m value for NADPH (*25*, *34*).

Y197S shows strong substrate inhibition at ≥200 μM GSSG. In contrast, wild-type GR is inhibited only at GSSG concentrations ≥2 mM. The lowered K_{mGSSG} value for Y197S and the increased inhibition by this substrate is expected for an enzyme which follows a kinetic ping-pong mechanism. From $[GSSG]_{min} = (K_{mGSSG}K_{iGSSG}[NADPH]/K_{mNADPH})^{1/2}$ (*39*), it follows that the minimum concentration of GSSG at which inhibition is observed decreases as the fixed NADPH concentration decreases. Assuming that K_{iGSSG} is unaffected by the mutation Y197S, this equation correctly predicts stronger substrate inhibition by GSSG for the mutant (K_m = 17 μM; see Table 1) than for the wild-type enzyme (K_m = 65 μM). The different K_m values can also, at least in part, explain why inhibition of Y197S by DNPG is much less pronounced when compared to wild type (Table 1). In wild-type GR, DNPG binds at the GSSG site as well as in a cavity at the 2-fold axis of the dimer. This additional site makes inhibition patterns difficult to interpret (*20*). Nonetheless, our data suggest that, other things being equal, the lowered K_{mGSSG} of Y197S may require a higher concentration of the DNPG as a competing inhibitor. Whether the mutation causes structural changes in either binding site of DNPG awaits X-ray diffraction analysis.

The Reductive Half-Reaction. The reaction of oxidized wild-type GR with NADPH proceeds in three phases following the very rapid formation of the NADPH−FAD charge-transfer complex, of which only the end can be observed. Hydride transfer from NADPH to the flavin is the first phase for which the rate can be measured. The resulting absorbance at 670 nm reflects the $FADH^-$−$NADP^+$ charge-transfer complex (Table 3). Its conversion to the thiolate−FAD charge-transfer complex in the second phase at a rate of approximately 100 s^{-1} results in decreased absorbance at 670 nm and increases at 540 and 463 nm. The long-wavelength absorbance of the thiolate−FAD charge-transfer complex is enhanced by excess NADPH as seen in the static titration (Table 2). The final phase may be due to equilibration between excess NADPH and $NADP^+$. The reductive half-reaction of Y114L is substantially the same as that of the wild-type enzyme.

In contrast, mutation of Tyr197 to a serine residue profoundly affects the reductive half-reaction. As seen in Figure 4, the NADPH−FAD charge-transfer complex (570 nm) and the $FADH^-$−$NADP^+$ charge-transfer complex (670 nm)—both at low levels—were maximal between 8 and 13 ms while flavin reduction continued to 60 ms. Because only 1 equiv of NADPH was used in the experiment shown in Figure 4, the final product would be a mixture of the free thiolate−FAD charge-transfer complex and a small amount of the thiolate−FAD charge-transfer complex with bound $NADP^+$ (Table 3). The rate of the reaction of Y197S with NADPH is some 15−20-fold slower than the reaction with wild-type enzyme. This accounts for the observed decrease in turnover. Both phases of reduction, hydride transfer from NADPH to FAD and passage of reducing equivalents from reduced flavin to the disulfide, are slowed by the mutation. The impact on the latter reaction is of interest because it supports the notion that the donor in this reaction is the complex between reduced flavin and pyridine nucleotide stabilized by the phenol ring of Tyr197.

The Oxidative Half-Reaction. The reaction of reduced wild-type GR with GSSG is monophasic. As discussed in the Results section, the reaction was followed as part of turnover in which enzyme reduction was achieved by 1 equiv of NADPH. There is no difficulty in separating the reduction (70 s^{-1} at 1 equiv of NADPH) and reoxidation phases given that the latter shows a dependence on the GSSG concentration with a limiting rate of 45 s^{-1}. The difference is even greater for Y114L where reoxidation occurs at a limiting rate of 11 s^{-1}. Protonation of GS^- II by His467′ is thought to be rate limiting in the oxidative half-reaction (*33*, *40*), and it is this reaction that we propose is promoted by the phenolate of Tyr114 (Scheme 2 in ref *16*). A partial negative charge on the phenol oxygen near the thiolate of GS^- II would assist its protonation.

Conclusions. The activity of Y197S is 17% that of the wild-type enzyme, indicating that Tyr197 is important but not crucial for enzyme activity. The rate of the limiting step in the reductive half-reaction, namely, the passage of reducing equivalents from the flavin to the disulfide, is decreased by approximately 95% relative to the wild-type enzyme. Remembering that the reductive half-reaction is only partially rate limiting, there is no inconsistency between this result and the decrease of 17% in the steady-state kinetics. The alteration of Tyr197 to a serine residue directly affects the interaction of the nicotinamide ring with the isoalloxazine ring. No enhancement of the thiolate−FAD charge-transfer complex by NADPH is observed in the absence of the phenol ring (Table 2). The mutation Y197S also decreases the K_m for GSSG as predicted for an enzyme operating by a ping-pong mechanism. The rate of the oxidative half-reaction is unaffected by the mutation. Mutation of Tyr114 to a leucine residue lowers the enzyme activity to 14% that of the wild-type enzyme, which indicates that this residue is involved but not essential in catalysis. The rate of reoxidation of reduced enzyme (EH_2) by GSSG is slowed to 27% relative to wild-type GR. Again, this comparison is for the oxidative half-reaction. It is suggested

that these are direct effects having their origin in a postulated synergism between the phenolate of Tyr114 and His467′. This histidine residue is the acid catalyst in the protonation of glutathione II, the first of two product molecules to dissociate. The rate of the reductive half-reaction is unaffected, and the K_m for NADPH is decreased as expected for a ping-pong enzyme. These findings further define the mechanism of glutathione reductase. In addition, they give clues to the catalytic specificity of glutathione reductase *in vivo*, that is, to the control of side reactions and to the suppression of the back-reaction. The results can be extended to other members of the pyridine nucleotide−disulfide oxidoreductase family that have or have not these tyrosine residues.

ACKNOWLEDGMENTS

The authors are grateful to Dr. Rowena G. Matthews, University of Michigan, and to Dr. P. Andrew Karplus, Cornell University, for helpful discussions. Dr. Uwe Bücheler, Heidelberg University, constructed the mutant GR species Y114L and Y197S. Dr. Alfonso Martinez, Max-Planck-Institut für Medizinische Forschung Heidelberg, provided Figures 1 and 2. The authors thank Ms. Donna M. Veine, Department of Veterans Affairs Medical Center, for expert help with the manuscript.

REFERENCES

1. Schirmer, R. H., Krauth-Siegel, R. L., and Schulz, G. E. (1989) in *Coenzymes and Cofactors* (Dolphin, D., Poulson, R., and Avramovic, O., Eds.) Vol. III, pp 553−596, John Wiley and Sons, New York.
2. Williams, C. H., Jr. (1992) in *Chemistry and Biochemistry of Flavoenzymes* (Müller, F., Ed.) Vol. III, pp 121−211, CRC Press, Boca Raton, FL.
3. Williams, C. H., Jr. (1976) in *The Enzymes* (Boyer, P. D., Ed.) Vol. XII, pp 89−173, Academic Press, New York.
4. Tutic, M., Lu, X., Schirmer, R. H., and Werner, D. (1990) *Eur. J. Biochem. 188*, 523−528.
5. Pai, E. F., and Schulz, G. E. (1983) *J. Biol. Chem. 258*, 1752−1757.
6. Pai, E. F., Karplus, P. A., and Schulz, G. E. (1988) *Biochemistry 27*, 4465−4474.
7. Karplus, P. A., and Schulz, G. E. (1989) *J. Mol. Biol. 210*, 163−180.
8. Karplus, P. A., and Schulz, G. E. (1987) *J. Mol. Biol. 195*, 701−729.
9. Greer, S., and Perham, R. N. (1986) *Biochemistry 25*, 2736−2742.
10. Nordhoff, A., Bücheler, U. S., Werner, D., and Schirmer, R. H. (1993) *Biochemistry 32*, 4060−4066.
11. Kunkel, T. A. (1985) *Proc. Natl. Acad. Sci. U.S.A. 82*, 488−492.
12. Sanger, F., Nicklen, S., and Coulson, A. R. (1977) *Proc. Natl. Acad. Sci. U.S.A. 74*, 5463−5467.
13. Worthington, D. J., and Rosemeyer, M. A. (1976) *Eur. J. Biochem. 67*, 231−238.
14. Krohne-Ehrich, G., Schirmer, R. H., and Untucht-Grau, R. (1977) *Eur. J. Biochem. 80*, 65−71.
15. Moroff, G., Ochs, R. S., and Brandt, K. G. (1976) *Arch. Biochem. Biophys. 173*, 42−49.
16. Rietveld, P., Arscott, L. D., Berry, A., Scrutton, N. S., Deonarain, M. P., Perham, R. N., and Williams, C. H., Jr. (1994) *Biochemistry 33*, 13888−13895.
17. Veine, D. M., Arscott, L. D., and Williams, C. H., Jr. (1994) in *Flavins and Flavoproteins 1993* (Yagi, K., Ed.) pp 497−500, Walter de Gruyter, Berlin and New York.
18. Clark, W. M. (1960) in *Oxidation−Reduction Potentials of Organic Systems*, p 490, Williams and Wilkins, Baltimore, MD.
19. Matthews, R. G. (1990) in *Flavins and Flavoproteins* (Curti, B., Ronchi, S., and Zanetti, G., Eds.) pp 593−597, Walter de Gruyter, Berlin and New York.
20. Bilzer, M., Krauth-Siegel, R. L., Schirmer, R. H., Akerboom, T. P. M., Sies, H., and Schulz, G. E. (1984) *Eur. J. Biochem. 138*, 373−378.
21. Arscott, L. D., Thorpe, C., and Williams, C. H., Jr. (1981) *Biochemistry 20*, 1513−1520.
22. Williams, C. H., Jr., Arscott, L. D., and Jones, E. T. (1976) *Flavins and Flavoproteins, Fifth International Symposium* (Singer, T. P., Ed.) pp 455−463, Elsevier Scientific Publishing Co., New York.
23. De Kok, A., and Visser, A. J. W. G. (1987) *FEBS Lett. 218*, 135−138.
24. Maeda-Yorita, K., Russell, G. C., Guest, J. R., Massey, V., and Williams, C. H., Jr. (1991) *Biochemistry 30*, 11788−11795.
25. Berry, A., Scrutton, N. S., and Perham, R. N. (1989) *Biochemistry 28*, 1264−1269.
26. Strickland, S., Palmer, G., and Massey, V. (1975) *J. Biol. Chem. 250*, 4048−4052.
27. Gassner, G. T., Johnson, D. A., Liu, H.-W., and Ballou, D. P. (1996) *Biochemistry 35*, 7752−7761.
28. Huber, P. W., and Brandt, K. G. (1980) *Biochemistry 19*, 4568−4575.
29. Arscott, L. D., Veine, D. M., and Williams, C. H., Jr. (1997) *Flavins and Flavoproteins 1996* (Stevenson, K. J., Massey, V., and Williams, C. H., Jr., Eds.) pp 679−682, University of Calgary Press, Calgary.
30. Schulz, G. E., Schirmer, R. H., Sachsenheimer, W., and Pai, E. F. (1978) *Nature 273*, 120−124.
31. Karplus, P. A., Pai, E. F., and Schulz, G. E. (1989) *Eur. J. Biochem. 178*, 693−703.
32. Wilkinson, K. D., and Williams, C. H., Jr. (1981) *J. Biol. Chem. 256*, 2307−2314.
33. Wong, K. K., Vanoni, M. A., and Blanchard, J. S. (1988) *Biochemistry 27*, 7091−7096.
34. Deonarain, M. P., Berry, A., Scrutton, N. S., and Perham, R. N. (1989) *Biochemistry 28*, 9602−9607.
35. Shaked, Z., Szajewski, R. P., and Whitesides, G. M. (1980) *Biochemistry 19*, 4156−4166.
36. Semenow-Garwood, D., and Garwood, D. C. (1972) *J. Org. Chem. 37*, 3804−3810.
37. Karshikoff, A., Reinemer, P., Huber, R., and Ladenstein, R. (1993) *Eur. J. Biochem. 215*, 663−670.
38. Xiao, G., Liu, S., Ji, X., Johnson, W. W., Chen, J., Parsons, J. F., Stevens, W. J., Gilliland, G. L., and Armstrong, R. N. (1996) *Biochemistry 35*, 4753−4765.
39. Segel, I. H. (1975) *Enzyme Kinetics: Behavior and Analysis of Rapid Equilibrium and Steady-State Enzyme Systems*, p 828, John Wiley and Sons, New York.
40. Wong, K. K., and Blanchard, J. S. (1989) *Biochemistry 28*, 3586−3590.

BI980637J